

SANDIA REPORT

SAND2017-6954
Unlimited Release
Printed July 2017

Smoothing Motion Estimates for Radar Motion Compensation

Armin W. Doerry

Prepared by
Sandia National Laboratories
Albuquerque, New Mexico 87185 and Livermore, California 94550

Sandia National Laboratories is a multission laboratory managed and operated by National Technology and Engineering Solutions of Sandia, LLC., a wholly owned subsidiary of Honeywell International, Inc., for the U.S. Department of Energy's National Nuclear Security Administration under contract DE-NA-0003525.

Approved for public release; further dissemination unlimited.



Sandia National Laboratories

Issued by Sandia National Laboratories, operated for the United States Department of Energy by Sandia Corporation.

NOTICE: This report was prepared as an account of work sponsored by an agency of the United States Government. Neither the United States Government, nor any agency thereof, nor any of their employees, nor any of their contractors, subcontractors, or their employees, make any warranty, express or implied, or assume any legal liability or responsibility for the accuracy, completeness, or usefulness of any information, apparatus, product, or process disclosed, or represent that its use would not infringe privately owned rights. Reference herein to any specific commercial product, process, or service by trade name, trademark, manufacturer, or otherwise, does not necessarily constitute or imply its endorsement, recommendation, or favoring by the United States Government, any agency thereof, or any of their contractors or subcontractors. The views and opinions expressed herein do not necessarily state or reflect those of the United States Government, any agency thereof, or any of their contractors.

Printed in the United States of America. This report has been reproduced directly from the best available copy.

Available to DOE and DOE contractors from

U.S. Department of Energy
Office of Scientific and Technical Information
P.O. Box 62
Oak Ridge, TN 37831

Telephone: (865) 576-8401
Facsimile: (865) 576-5728
E-Mail: reports@adonis.osti.gov
Online ordering: <http://www.osti.gov/bridge>

Available to the public from

U.S. Department of Commerce
National Technical Information Service
5285 Port Royal Rd.
Springfield, VA 22161

Telephone: (800) 553-6847
Facsimile: (703) 605-6900
E-Mail: orders@ntis.fedworld.gov
Online order: <http://www.ntis.gov/help/ordermethods.asp?loc=7-4-0#online>



SAND2017-6954
Unlimited Release
Printed July 2017

Smoothing Motion Estimates for Radar Motion Compensation

Armin W. Doerry
ISR Mission Engineering
Sandia National Laboratories
PO Box 5800
Albuquerque, NM 87185-0519

Abstract

Simple motion models for complex motion environments are often not adequate for keeping radar data coherent. Even perfect motion samples applied to imperfect models may lead to interim calculations exhibiting errors that lead to degraded processing results. Herein we discuss a specific issue involving calculating motion for groups of pulses, with measurements only available at pulse-group boundaries.

Acknowledgements

This report was funded by General Atomics Aeronautical Systems, Inc. (GA-ASI) Mission Systems under Cooperative Research and Development Agreement (CRADA) SC08/01749 between Sandia National Laboratories and GA-ASI.

General Atomics Aeronautical Systems, Inc. (GA-ASI), an affiliate of privately-held General Atomics, is a leading manufacturer of Remotely Piloted Aircraft (RPA) systems, radars, and electro-optic and related mission systems, including the Predator®/Gray Eagle®-series and Lynx® Multi-mode Radar.

Contents

| | |
|---|----|
| Foreword | 6 |
| Classification..... | 6 |
| 1 Introduction | 7 |
| 2 Background – The Problem..... | 9 |
| 3 Mitigation | 13 |
| 3.1 Simple Scheme | 13 |
| 3.2 Better Scheme..... | 16 |
| 3.3 Further Improvements | 19 |
| 3.3.1 Shorter Pulse Groups..... | 19 |
| 3.3.2 Better Motion Model | 19 |
| 3.3.3 More Exotic Techniques..... | 21 |
| 4 Conclusions and Final Comments | 23 |
| References | 25 |
| Distribution..... | 26 |

Foreword

This report details the results of an academic study. It does not presently exemplify any modes, methodologies, or techniques employed by any operational system known to the author.

Classification

The specific mathematics and algorithms presented herein do not bear any release restrictions or distribution limitations.

This report formalizes preexisting informal notes and other documentation on the subject matter herein.

1 Introduction

Many radar modes require data to be collected in a manner to maintain pulse-to-pulse target-response coherence. Proper radar configuration then requires some degree of knowledge of expected target range and range variations over a Coherent Processing Interval (CPI) of pulses. For Synthetic Aperture Radar (SAR), the CPI is in fact the synthetic aperture. For Inverse-SAR (ISAR) this might be the entire dwell. Correcting radar data for range variations is termed “Motion Compensation.”

In many cases, knowledge of range and range-rate (velocity) between radar and target is sufficient for proper coherent processing. However, even when these are not precisely known, we still presume some degree of “smoothness” in the range variations, implying smooth and relatively small variations in velocity during the CPI. Indeed, many radar modes in fact presume constant velocity. However, this is not always the case.

Herein we investigate a very specific problem, namely the case of complex relative motion being represented with an incomplete set of range and velocity measurements. That is, we investigate suitable means to estimate range and velocity in-between perhaps somewhat sparse measurement times.

This report is not about improving the accuracy of any motion measurement subsystem, but rather about how best to use those measurements for sample times other than those specifically associated with the motion data.

For this report we will presume that a CPI is divided into pulse groups, and within an individual pulse group the relative motion is modelled with a single reference range and constant velocity for calculating any range offsets within the pulse-group. Any higher-order motion such as accelerations during the pulse group will cause an error in the range profile. Even if the next pulse group were to receive perfect new range and velocity measures, the resulting radar data might exhibit a range-profile discontinuity at the pulse-group boundary. This often manifests in processed data as undesirable low-level sidelobes. This report is about adjusting parameters to reduce the objectionable sidelobes in the processed data.

“Don't be afraid to see what you see.”
-- Ronald Reagan

2 Background – The Problem

To set up the following discussion, we begin by defining a generic range profile function

$$r(t) = \text{continuous function of time } t. \quad (1)$$

The phase of a radar echo signal is then modelled as

$$\Phi(t) = \frac{4\pi}{\lambda} r(t) = \text{radar echo phase function}, \quad (2)$$

where

$$\lambda = \text{radar nominal wavelength}. \quad (3)$$

We will sample the signal at discrete times

$$t = T_p m, \quad (4)$$

where

$$\begin{aligned} T_p &= \text{Pulse Repetition Interval (PRI), presumed constant, and} \\ m &= \text{integer pulse index, } 0 \leq m \leq M - 1. \end{aligned} \quad (5)$$

We will now parse the pulse samples into contiguous nonoverlapping groups, and define new indices as

$$m = nP + p, \quad (6)$$

where

$$\begin{aligned} n &= \text{integer pulse-group index, } 0 \leq n \leq N - 1, \text{ and} \\ p &= \text{integer index within a pulse group, } 0 \leq p \leq P - 1. \end{aligned} \quad (7)$$

This makes the sample times at discrete values

$$t = T_p (nP + p). \quad (8)$$

The sampled ranges are now identified with the new sample nomenclature as

$$r_{n,p} = r(T_p (nP + p)) = r(T_p Pn + T_p p). \quad (9)$$

We will make the reasonable assumption that the range function is analytic. This allows us to expand the range function into a Taylor series as

$$r(t) = \sum_{i=0}^{\infty} \frac{r^{(i)}(t_0)}{i!} (t-t_0)^i, \quad (10)$$

where

$$\begin{aligned} t_0 &= \text{arbitrary reference time, and} \\ i &= \text{integer index value.} \end{aligned} \quad (11)$$

A first order approximation based on Eq. (10) is then

$$r(t) \approx r(t_0) + v(t_0)(t-t_0), \quad (12)$$

where we define the velocity as

$$v(t) = \frac{d}{dt} r(t). \quad (13)$$

If we equate the reference time to the beginning of a pulse group as

$$t_0 = T_p P n. \quad (14)$$

then we may approximate the sampled ranges as

$$r_{n,p} \approx r_{n,0} + v_{n,0}(T_p p), \quad (15)$$

where the sampled velocity is identified as

$$v_{n,p} = v(T_p P n + T_p p). \quad (16)$$

Of course, Eq. (15) being an approximation, we may define a corresponding range error as

$$\varepsilon_{n,p} = r_{n,0} + v_{n,0}(T_p p) - r_{n,p}. \quad (17)$$

Ideally, we wish this error to be negligible. However, even with perfect measurements of sampled motion parameters $r_{n,0}$ and $v_{n,0}$, we cannot guarantee this. Furthermore, even if Eq. (15) were exact, we would generally need to allow for some error or inconsistency in values for $r_{n,0}$ and $v_{n,0}$.

For a radar echo, the range error generates a phase error calculated as

$$\phi_{\varepsilon,n,p} = \frac{4\pi}{\lambda} \varepsilon_{n,p} . \quad (18)$$

With this phase, an error signal is calculated as

$$s_{\varepsilon,n,p} = e^{j\phi_{\varepsilon,n,p}} . \quad (19)$$

The impact of this phase error on the signal spectrum is calculated by a Discrete-time Fourier Transform (DFT) as

$$X_{\varepsilon}(f) = \sum_{m=0}^{M-1} s_{\varepsilon,n,p} e^{-j2\pi f T_p m} , \quad (20)$$

where we recall the indices are related by Eq. (6).

If we include a window taper function for sidelobe control, we may calculate the spectrum as

$$X_{\varepsilon}(f) = \sum_{m=0}^{M-1} s_{\varepsilon,n,p} w_m e^{-j2\pi f T_p m} , \quad (21)$$

where

$$w_m = \text{the coefficients of your favorite window taper function.}^1 \quad (22)$$

We illustrate all this with an example.

Example #1

Consider a Ku-band radar operating with the following parameters.

$$\begin{aligned} \lambda &= 0.018 \text{ m,} \\ f_p &= 1000 \text{ Hz,} \\ M &= 1024 \text{ samples, these parsed into} \\ P &= 32 \text{ samples, and} \\ N &= 32 \text{ sample groups.} \end{aligned} \quad (23)$$

We exemplify notional radar range variations with a half-cycle of a sinusoid, with amplitude of 0.5 m. Figure 1 illustrates the motion “truth” as well as the basic estimated motion using Eq. (15). The range error is illustrated in Figure 2. Note that within a pulse group, the error grows until the beginning of the next pulse group. This causes the spectrum to exhibit sidelobe “spikes” as illustrated in Figure 3.

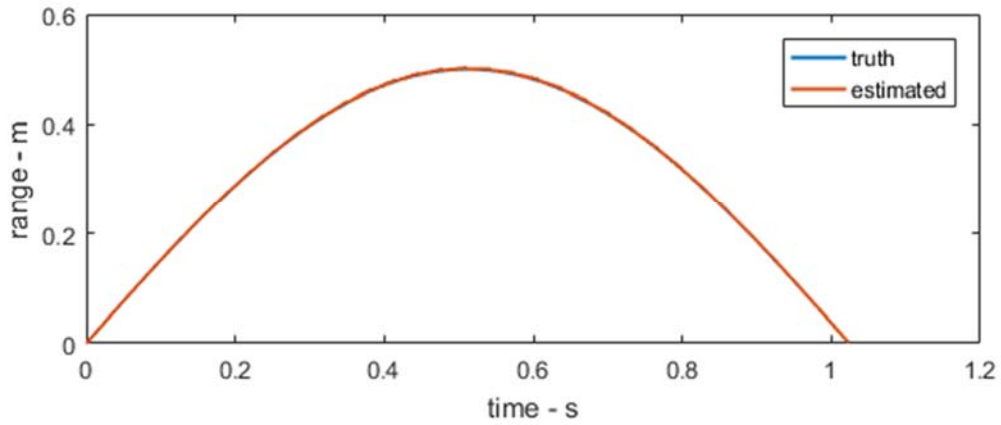


Figure 1. Example #1 -- Truth and basic estimated range functions.

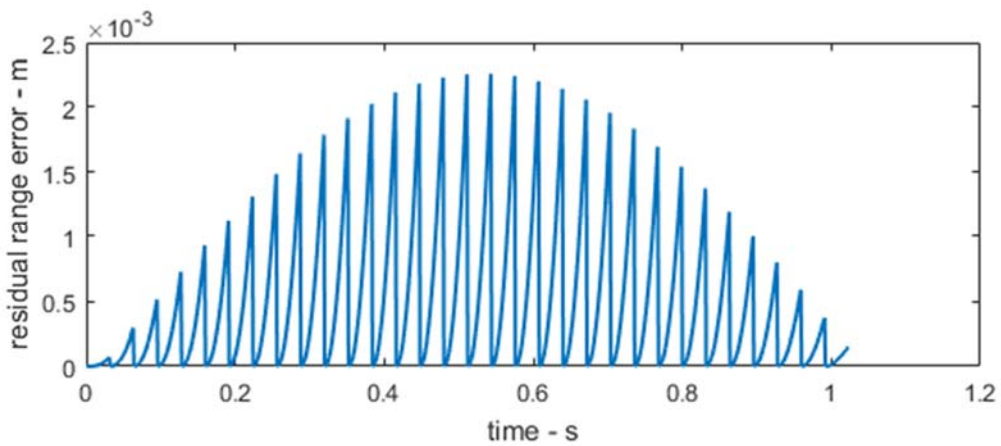


Figure 2. Example #1 -- Error between basic estimated and true range functions.

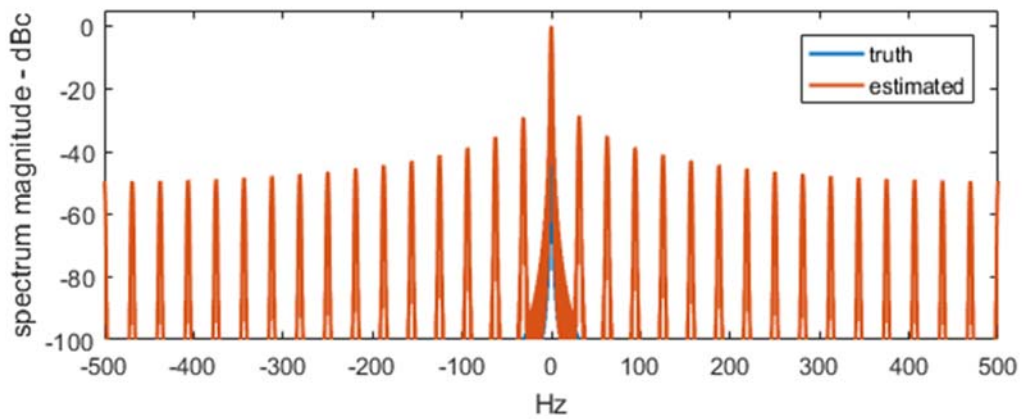


Figure 3. Example #1 -- Spectrum of the error between signals using basic estimated and true ranges. A Hann window taper function was used for processing sidelobe control.

Discussion

The “spikey” sidelobes evident in Figure 3 are problematic in that they may generate false alarms and otherwise reduce sensitivity to target detections and characterization. We don’t like this. These exist because of the magnitude and regularity of the discontinuities in the range error evident in Figure 2. Reducing the spikey sidelobes requires us to reduce the magnitude or regularity of the discontinuities. Herein we will focus on reducing the magnitude of the discontinuities.

In summary, we desire a simple algorithm to improve the spectral sidelobes of the error signal based on range and velocity estimates, perhaps even at the expense of accuracy and precision of the range estimate.

3 Mitigation

3.1 Simple Scheme

At issue are the sidelobes in Figure 3. These are due to the unexpected range jumps (discontinuities) between pulse groups. Specifically, these are due to the fact that generally

$$r_{n+1,0} \neq (r_{n,0} + v_{n,0}T_pP). \quad (24)$$

One answer is to force Eq. (24) to be an equality. That is, we identify and use the estimates

$$\begin{aligned} \hat{r}_{0,0} &= r_{0,0}, \text{ and} \\ \hat{r}_{n+1,0} &= (\hat{r}_{n,0} + v_{n,0}T_pP). \end{aligned} \quad (25)$$

Essentially, we use an initial measurement of range, and thereafter update new estimates of range by summing (integrating) only measurements of velocity.

More specifically, we rearrange a bit and use the range estimates

$$\begin{aligned} \hat{r}_{0,0} &= r_{0,0}, \\ \hat{r}_{n,0} \Big|_{n>0} &= (\hat{r}_{n-1,0} + v_{n-1,0}T_pP), \text{ and} \\ \hat{r}_{n,p} &= (\hat{r}_{n,0} + v_{n,0}T_pP). \end{aligned} \quad (26)$$

While we may expect range errors will grow with time, at least the pesky discontinuities will have been reduced, thereby reducing the problematic sidelobes.

Example #2

We repeat Example #1 except that now estimated ranges use Eq. (26). Figure 4 shows a smoother range estimate, but exhibiting a growing error. The range error is explicitly illustrated in Figure 5, which clearly shows the growth in net error, even as the jumps are diminished. Nevertheless, Figure 6 clearly shows a reduction in the spikey sidelobes, as desired, with even the nearest sidelobes reduced by more than 10 dB. However, for this example, the nature of the residual range error causes a shift and degradation of the mainlobe as shown in Figure 7.

Discussion

Figure 5 clearly shows that the range estimate is now continuous, which is good. However, also evident is that the slope of the range function, i.e. velocity, remains not continuous. This discontinuity of the velocity is ultimately the cause for the remaining spikey sidelobes in Figure 6.

While Figure 6 clearly shows a desirable reduction in sidelobes, Figure 7 shows an undesirable shift and degradation of the main spectral peak. This is due to the gross overall range error variation illustrated in Figure 5. Note that there is an overall linear component, and large cubic component to the range error, for which the shift and degradation of the spectral peak is entirely consistent.² For many applications, this shift and degradation is quite tolerable, especially if the net range error is less than the range resolution of the radar. In these cases, if necessary, a simple autofocus can reduce the effects of the higher-order range errors. Otherwise, for larger range errors, more exotic autofocus operations might be required.³

In summary, estimating range based on velocity alone can reduce the undesired spectral sidelobes of the phase function, but may come at a price of degrading the spectral mainlobe response. We now further desire a still-simple algorithm to improve the spectral sidelobes of the error signal based on range and velocity estimates, but without the shifting and degradation of the mainlobe response.

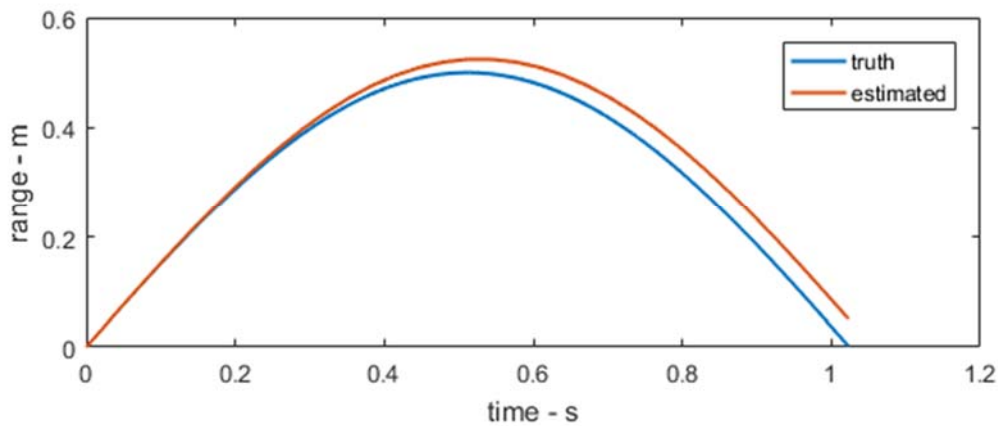


Figure 4. Example #2 -- Truth and improved estimated range functions.

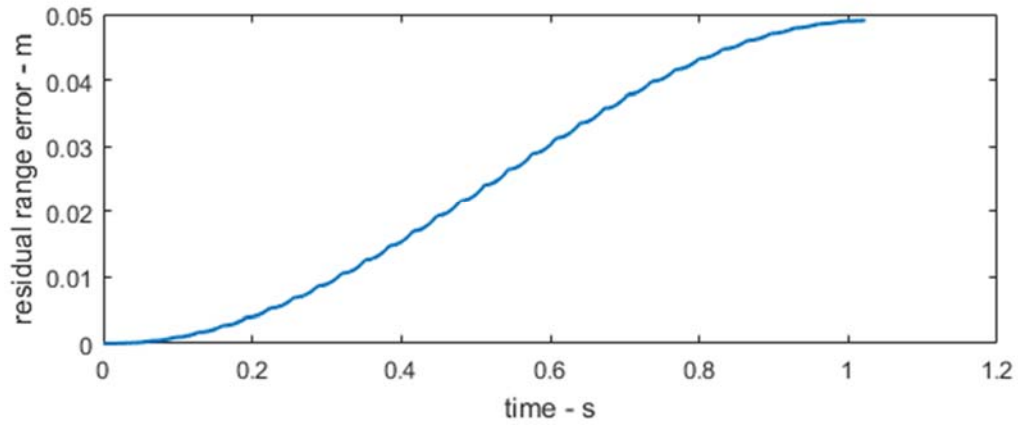


Figure 5. Example #2 -- Error between improved estimated and true range functions.

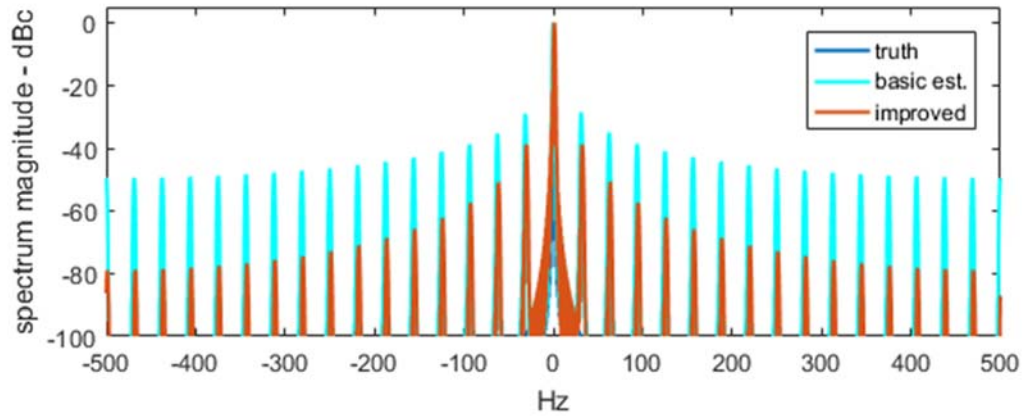


Figure 6. Example #2 -- Spectrum of the error between signals using improved estimated, basic estimated, and true ranges. A Hann window taper function was used for processing sidelobe control.

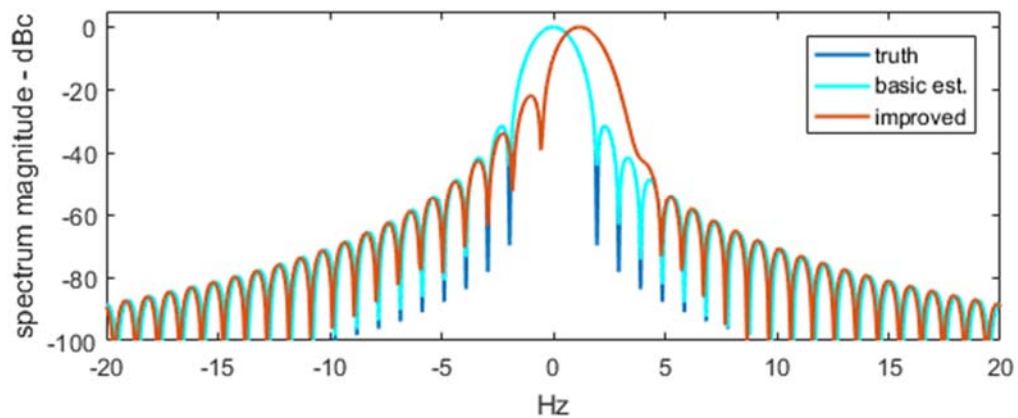


Figure 7. Example #2 -- Zoom of mainlobe of Figure 6.

3.2 Better Scheme

At issue is the growing range error in Figure 4 and Figure 5. This is due to the estimated range at the start of the next pulse group (using accumulated velocities) differing from the actual measured range. Specifically, these are due to the fact that for Eq. (26) generally

$$r_{n,0} \neq \hat{r}_{n,0} \quad \text{for } n > 0. \quad (27)$$

One answer is to force Eq. (27) to be an equality, but while retaining the benefits of integrating/accumulating velocity. We do this by modifying our estimated velocity. That is, we identify and use the estimates

$$\begin{aligned} \hat{r}_{0,0} &= r_{0,0}, \\ \hat{v}_{n,0} &= v_{n,0} + \frac{r_{n,0} - \hat{r}_{n,0}}{T_p P}, \text{ and} \\ \hat{r}_{n+1,0} &= (\hat{r}_{n,0} + \hat{v}_{n,0} T_p P). \end{aligned} \quad (28)$$

This forces the desired incorporation of the next range estimate being an offset from the previous range measurement using a velocity measurement, namely this equates to

$$\hat{r}_{n+1,0} = r_{n,0} + v_{n,0} T_p P. \quad (29)$$

In this manner, the range error does not accumulate for more than a single pulse group. However, rearranging a bit, the individual range estimates within a pulse group are now calculated as

$$\begin{aligned} \hat{r}_{0,0} &= r_{0,0}, \\ \hat{r}_{n,0} \Big|_{n>0} &= (\hat{r}_{n-1,0} + \hat{v}_{n-1,0} T_p P), \\ \hat{v}_{n,0} &= v_{n,0} + \frac{r_{n,0} - \hat{r}_{n,0}}{T_p P}, \text{ and} \\ \hat{r}_{n,p} &= (\hat{r}_{n,0} + \hat{v}_{n,0} T_p p). \end{aligned} \quad (30)$$

Nevertheless, while we may expect range errors to be bounded, the pesky discontinuities still exist but also still at the reduced level.

Example #3

We repeat Example #1 except that now estimated ranges use Eq. (30). Figure 8 shows a smoother range estimate, but exhibiting no growing error. The range error is explicitly illustrated in Figure 9, which clearly shows the limited growth in net error, with the jumps still diminished. Figure 10 clearly still shows a reduction in the spikey sidelobes, as desired, with the nearest sidelobes still reduced by more than 10 dB. However, for this example, Figure 11 shows that the shift and degradation of the mainlobe previously shown in Figure 7 has been mitigated.

Discussion

Figure 9 continues to show that the range estimate is still continuous, which is good. It also still shows that the slope of the range function, i.e. velocity, remains not continuous; still the cause for the remaining spikey sidelobes in Figure 10.

However, Figure 11 clearly shows that the previous undesirable shift and degradation of the main spectral peak has been mitigated, due to the diminishment of the previous gross overall range error variation.

In summary, estimating range based on velocity alone can reduce the undesired spectral sidelobes of the phase function, but may come at a price of degrading the spectral mainlobe response. However, a modification to the velocity estimate used in updating range can reduce and bound the overall range error, thereby correcting the conditions that led to mainlobe degradation and shift.

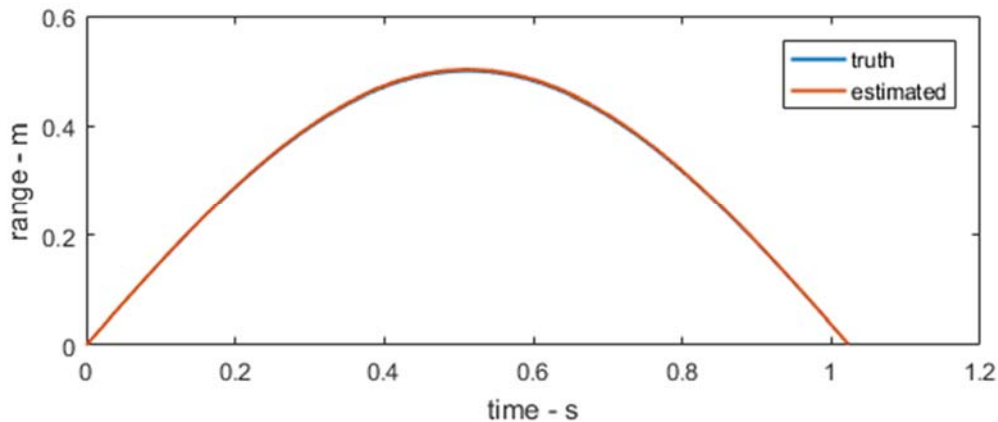


Figure 8. Example #3 -- Truth and improved estimated range functions.

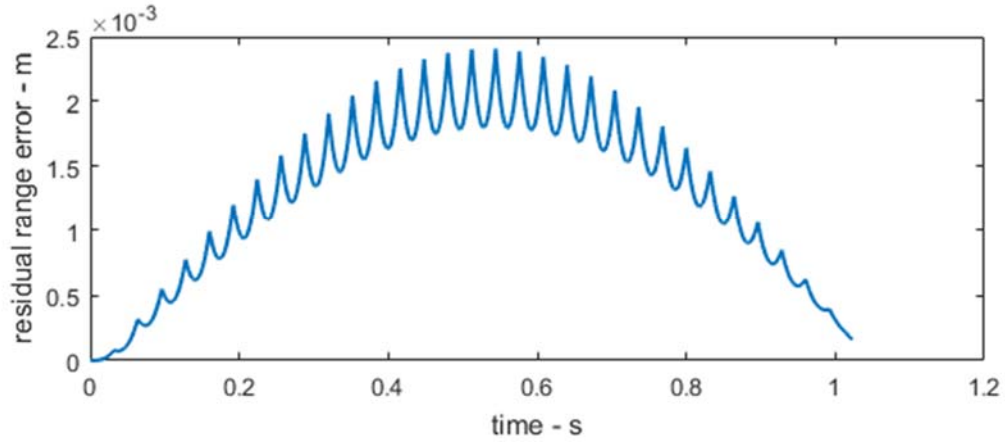


Figure 9. Example #3 -- Error between improved estimated and true range functions.

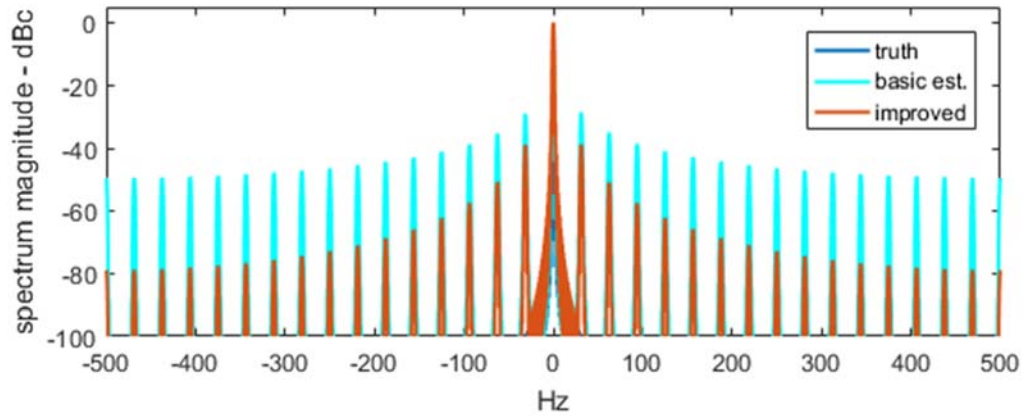


Figure 10. Example #3 -- Spectrum of the error between signals using improved estimated, basic estimated, and true ranges. A Hann window taper function was used for processing sidelobe control.

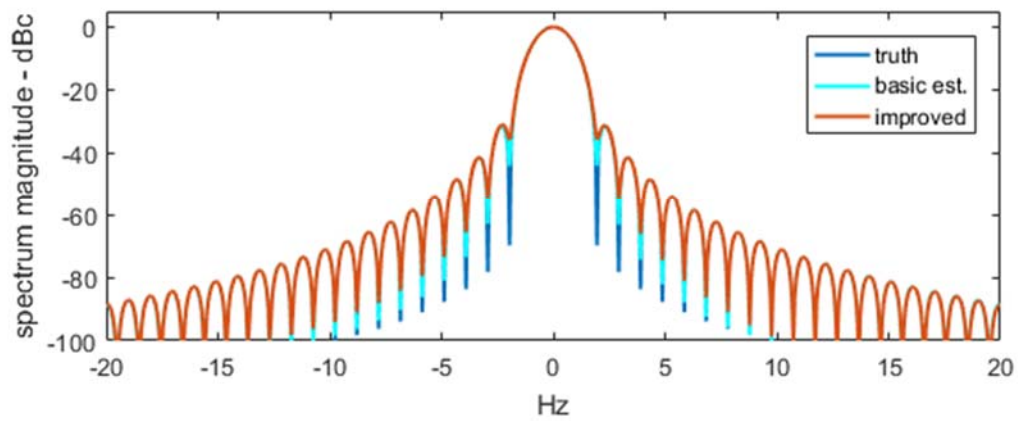


Figure 11. Example #3 -- Zoom of mainlobe of Figure 10.

3.3 Further Improvements

Further improvement with respect to Example #3 requires us to further mitigate the offending nature of the range estimate error. Reducing the spikey sidelobes in Figure 10 requires us to smooth even more the range error in Figure 9. We may do this in any of several manners.

3.3.1 Shorter Pulse Groups

One mechanism to limit the growth of range estimate error is to perform the estimate more often, that is, use shorter pulse groups. We illustrate with an example.

Example #4

We repeat Example #3 except we limit the pulse group to $P = 8$, thereby growing to $N = 128$. Note in Figure 12 that the peak range error has diminished by more than an order of magnitude, and in Figure 13 the sidelobes have also reduced, as well as spread.

Discussion

As a pulse group shortens, there is less time for a linear prediction of range to deviate from true, thereby manifesting a smaller net range error. In the limit, each pulse is its own group, and no prediction is necessary since range is measured for each pulse. While optimum, this is often not realizable in real-time hardware and software. Nevertheless, to the extent possible, the length of a pulse group should perhaps be kept to a minimum.

3.3.2 Better Motion Model

Heretofore we have employed a first-order motion model for predicting range within a pulse group. An arguably better model might also include an acceleration term, as perhaps

$$\hat{r}_{n,p} = \hat{r}_{n,0} + \hat{v}_{n,0}(T_p p) + \frac{\hat{a}_{n,0}}{2}(T_p p)^2, \quad (31)$$

where

$$\hat{a}_{n,0} = \text{an estimate of the acceleration.} \quad (32)$$

Recall that acceleration is the time-rate-of-change of velocity.

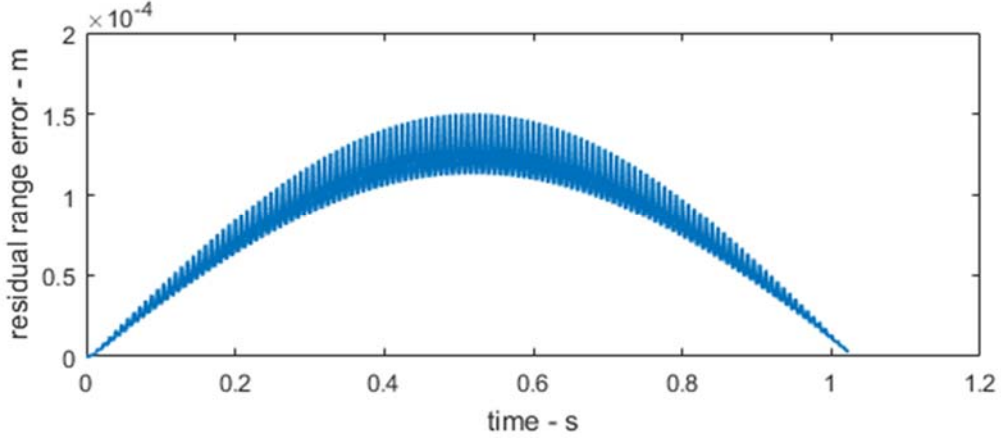


Figure 12. Example #4 -- Error between improved estimated and true range functions.

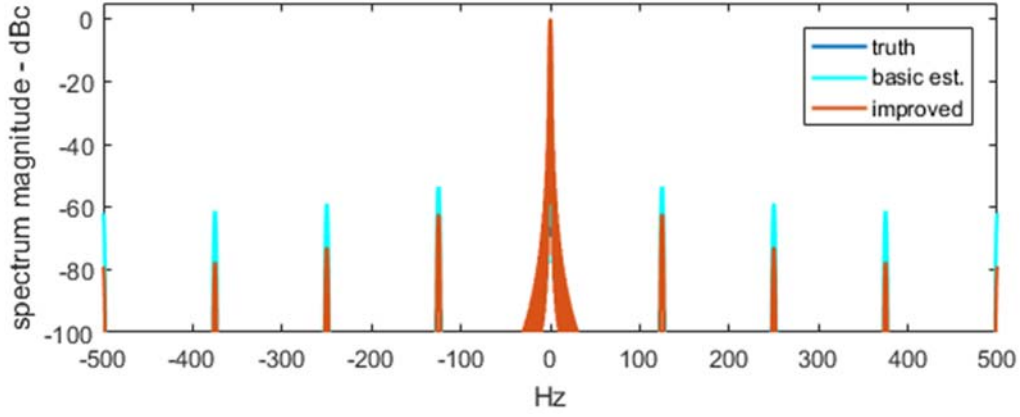


Figure 13. Example #4 -- Spectrum of the error between signals using improved estimated, basic estimated, and true ranges. A Hann window taper function was used for processing sidelobe control.

In this case where acceleration information is available, without elaboration, and ignoring how we might estimate acceleration, we employ the equations

$$\begin{aligned}
 \hat{r}_{0,0} &= r_{0,0}, \\
 \hat{r}_{n,0} \Big|_{n>0} &= \hat{r}_{n-1,0} + \hat{v}_{n-1,0} T_p P + \hat{a}_{n-1,0} (T_p P)^2, \\
 \hat{v}_{n,0} &= v_{n,0} + \frac{r_{n,0} - \hat{r}_{n,0}}{T_p P}, \text{ and} \\
 \hat{r}_{n,p} &= \hat{r}_{n,0} + \hat{v}_{n,0} T_p p + \hat{a}_{n,0} (T_p p)^2.
 \end{aligned} \tag{33}$$

We illustrate with an example.

Example #5

We repeat Example #3 except we now allow employing an acceleration measurement to be included in the range function estimate. In this case we allow the acceleration estimate in Eq. (33) to be an actual measured value, which we assume is “truth.” That is, we let

$$\hat{a}_{n,0} = a_{n,0} = \frac{d^2}{dt^2} r(t). \quad (34)$$

We observe in Figure 15 that the objectionable sidelobes have therewith been substantially reduced.

Discussion

Since a fundamental property of analytic functions is that if we know the function value and all its derivatives at a single point, then we know the entire function everywhere. Consequently, knowledge of higher order motion terms generally allows us to better estimate the range function during a pulse group. Even just the second order term (acceleration) helps us significantly. The result of a higher-fidelity motion prediction is to reduce the objectionable sidelobes in the signal spectrum. This is a good thing.

We concede that we have ignored the question “How good does the acceleration estimate need to be?” We shall not explore this here. We will stipulate that motion estimates will need to operate with information that is available. If a high-quality acceleration measurement is available, then it might perhaps be considered for employment. The final decision must also consider just how low sidelobes need to be suppressed. This is a system design issue.

3.3.3 More Exotic Techniques

It is clear that in order to estimate velocities to be consistent with range changes, that we are employing predictive filtering for the range. This suggests that more elaborate filters across a longer history of pulses might be advantageous; perhaps in the form of an Auto-Regressive Moving-Average (ARMA) filter, or even a Kalman filter of some sort.

The system designer will need to evaluate whether the added complexity of these filters merits the improvement that they might offer. We will forego any further investigation of these in this report.

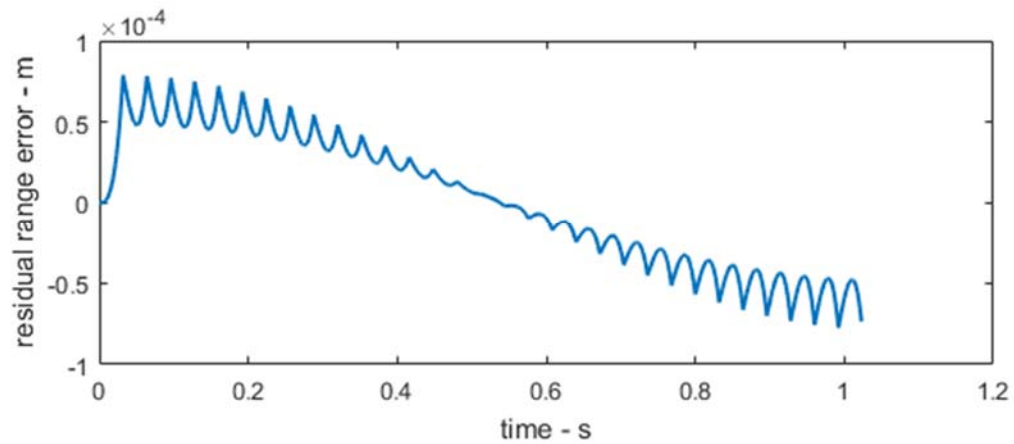


Figure 14. Example #5 -- Error between improved estimated and true range functions.

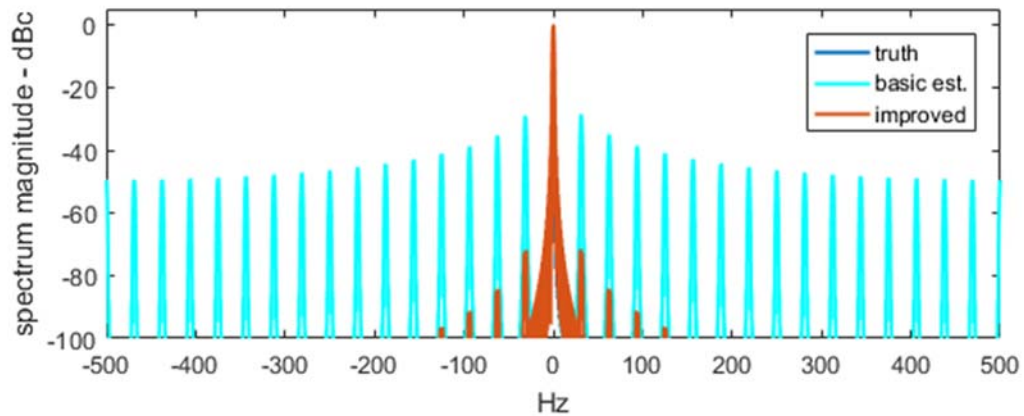


Figure 15. Example #5 -- Spectrum of the error between signals using improved estimated, basic estimated, and true ranges. A Hann window taper function was used for processing sidelobe control.

4 Conclusions and Final Comments

We reiterate the following key points.

- Even perfect motion measurements, when applied to imperfect motion models, may manifest as degraded radar data coherence from pulse to pulse.
- Degraded coherence may result from discontinuities in the calculated motion model between radar and target, especially as the model accumulates errors between actual measurements. These discontinuities may result in elevated and “spikey” sidelobes in the processed output.
- This degradation may be reduced by adjusting range and velocity measurements before calculating motion parameter between measurements. Several algorithms were discussed for doing so.

We further make the following comment.

- Herein we have identified velocity as the rate-of-change of the range. Consequently, for the equations developed herein an increasing range yields a positive range-rate; a positive velocity. We are cognizant that many radar systems define a line-of-sight velocity as a closing range-rate, that is, an increasing range yields a negative line-of-sight velocity. For these systems, care should be taken that the proper sign is accounted when using line-of-sight velocity in place of range-rate parameter $v_{n,p}$.

*“A child of five would understand this.
Send someone to fetch a child of five.”
-- Groucho Marx*

References

- ¹ Armin W. Doerry, *Catalog of Window Taper Functions for Sidelobe Control*, Sandia National Laboratories Report SAND2017-4042, Unlimited Release, April 2017.
- ² Armin W. Doerry, *Anatomy of a SAR Impulse Response*, Sandia National Laboratories Report SAND2007-5042, Unlimited Release, August 2007.
- ³ Armin W. Doerry, *Autofocus Correction of Excessive Migration in Synthetic Aperture Radar Images*, Sandia National Laboratories Report SAND2004-4770, September 2004.

Distribution

Unlimited Release

| | | | |
|---|---------|-------------------|------------------------|
| 1 | MS 0519 | M. R. Lewis | 5349 |
| 1 | MS 0519 | A. W. Doerry | 5349 |
| 1 | MS 0519 | L. Klein | 5349 |
| 1 | MS 0532 | S. P. Castillo | 5340 |
| 1 | MS 0899 | Technical Library | 9536 (electronic copy) |

